Urban Forestry & Urban Greening 113 (2025) 129090

Contents lists available at ScienceDirect

Urban Forestry & Urban Greening

journal homepage: www.elsevier.com/locate/ufug

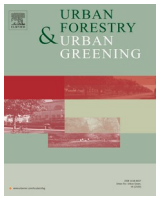

Original article

Phenological description of *Ailanthus altissima* (Mill.) Swingle using the BBCH-scale: Groundwork for developing strategies to control invasive species and mitigate potential allergy risks

Jorge Romero-Morte [a,*], Gonzalo Ortiz de Elguea-Culebras [b]

[a] Department of Pharmacology, Pharmacognosy and Botany, Faculty of Pharmacy, Complutense University of Madrid, Ramón y Cajal Square, Madrid 28040, Spain
[b] Department of Agronomy and Phytochemistry of Medicinal and Aromatic Plants, Agroforestry Research Center of Albaladejito (CIAF), Regional Institute of Agri-Food and Forestry Research and Development of Castilla-La Mancha (IRIAF), N-310, 19, Ciudad Real, Tomelloso 13700, Spain

ARTICLE INFO

Keywords:
Ailanthus altissima
Phenology
BBCH-scale
Invasive Species Management
Allergic Risks

ABSTRACT

Alien species pose a growing threat to biodiversity and ecosystems due to their capacity to establish and proliferate beyond their native ranges. Among them, *Ailanthus altissima* (Mill.) Swingle ranks among the most concerning species globally, especially across the Mediterranean basin, where its spread continues to intensify. Native to China and northern Vietnam, this tree has been widely introduced for ornamental purposes. Its invasive success facilitates the displacement of native flora, disruption of ecological processes, and significant impacts on public health due to its allergenic potential, including in urban areas. This study applies the BBCH-scale to describe the full phenological cycle of a population in Cuenca (Spain). A total of 20 adult individuals were monitored (10 males and 10 females) leading to identify 8 of the 10 main BBCH-scale stages and 41 secondary stages, covering the entire cycle from bud emergence to leaf senescence, while linear interpolation was used for the temporal analysis of stage duration. Additionally, statistical comparisons between sexes were conducted using one-way ANOVA with post-hoc Tukey HSD test, while Pearson's correlation analysis assessed to correlate these patterns with meteorological conditions, highlighting the influence of key meteorological variables (temperature, relative humidity, insolation and precipitation) on phenophase timing. These findings demonstrate that the BBCH-scale offers a precise framework to monitor phenology in this species, supporting improved management of invasive populations and enabling better forecasting of pollen release, crucial for public health monitoring in areas with high allergy incidence.

1. Introduction

Alien species, characterized by their ability to establish and proliferate beyond their native areas, represent broad and complex negative ecological impacts. These include alteration of vegetation structures, biogeochemical cycles and soil regeneration processes, negatively affecting biodiversity and essential ecosystem services (Simberloff et al., 2013; Vilà et al., 2024), which are key contributors to global change (Pyšek et al., 2020). Furthermore, Simberloff et al. (2013) and Vilà et al. (2024) reported that their expansion is exacerbated by globalization related mainly to international trade, causing the colonization of new territories and the displacement of native species. This also has negative consequences in various habitats, including urban areas, where invasive species can affect biodiversity and human health, making their management a global priority.

The Tree of Heaven or *Ailanthus altissima* (Mill.) Swingle has historically been used in traditional Asian medicine for human well-being, exhibiting antitumoral, antiviral, insecticidal and herbicidal properties (Caramelo et al., 2021; De Martino and De Feo, 2008). Additionally, its fibers have demonstrated to produce good quality paper (Baptista et al., 2014). However, its current primary use as an ornamental plant has promoted its status as one of the most widespread invasive species globally (Sladonja et al., 2015), with noticeable impacts in Europe and, especially, in the Mediterranean basin (Motti et al., 2021). Besides, its range continues to increase and is projected to increase in the coming years (Puchałka et al., 2023). In view of the magnitude of the effects generated, this species has been included in the list of Invasive Alien Species (IAS) of Union concern under the EU Regulation 143/2014

* Corresponding author.
E-mail addresses: jromer09@ucm.es (J. Romero-Morte), gonzaloo@jccm.es (G.O. de Elguea-Culebras).

https://doi.org/10.1016/j.ufug.2025.129090
Received 8 May 2025; Received in revised form 14 August 2025; Accepted 29 September 2025
Available online 1 October 2025

(European Commission, 2020). The invasiveness of this plant is partially exacerbated by the combination of sexual and asexual reproduction strategies. It is suggested that each individual is capable of producing over 325,000 seeds annually, while the germination success rate is estimated at around 98 % (Kowarik and Säumel, 2007). These seeds are well-adapted for dispersal by wind and water, thus enabling a broad and rapid distribution. Furthermore, its ability to regenerate from cut roots and stumps, along with its negative allelopathic mechanisms, provides further competitive advantages in invaded habitats (Sladonja et al., 2015). Despite requiring warm and humid climates with rainfall exceeding 500 mm/year, it also exhibits remarkable tolerance to extreme conditions, including drought, frost or pollution. Such capacity enables it to thrive in harsh environments, even offering favourable conditions for its growth (Constán-Nava et al., 2010). Thus, Kowarik and Säumel (2007) reviewed that despite seedlings are severely affected by frosts, adult trees withstand temperatures as low as −33°C. However, due to high seed production and rapid reproductive maturity resulting in high propagule pressure, some seedlings survive and enable the species to spread into cooler climates. For instance, Paź-Dyderska et al., (2020) report the expansion of *Ailanthus altissima* in urban areas of Poland, at the cooler edge of its range, facilitated by recent climate warming. This resilience also allows this plant to colonize a wide range of habitats after environmental disturbances such as fires or soil degradation from anthropogenic activities (i.e. construction, mining, abandoned agricultural land, etc). Finally, it is reported that the presence of *A. altissima* in urban and peri-urban areas (Constán-Nava et al., 2010) may cause adverse health effects, including respiratory allergies and dermatitis (Ballero et al., 2003; Werchan et al., 2024).

In this sense, it is essential to delve into the understanding of the phenological cycle of *A. altissima* for the further development of effective management and control strategies, which consists of systematically monitoring the biological stages of a plant throughout its life cycle (Schwartz, 2013). This approach was initially developed for tracking the growth and development of cereal crops (Zadoks et al., 1974) and later standardized by Meier (2001) through the BBCH-scale, while enabling the comparison of phenological data along studies and regions. Although this scale was initially intended to codify the phenological stages of plant species of agronomic interest, such as olive (Rojo and Pérez-Badia, 2014) or mango (Delgado et al., 2011), in recent years, the BBCH-scale has also been applied in the assessment of a wide array of plants. This also comprises invasive species, such as *Parthenium hysterophorus* (Kaur et al., 2017), *Broussonetia papyrifera* (Maan et al., 2020), *Lantana camara* (Kumar et al., 2022) or *Sapium sebiferum* (Jaryan et al., 2014). Such assessments may lead to the development of phenological calendars as well as determining optimal times for the implementation of control measures. Although there are some studies on the phenology of *A. altissima* (Werchan et al., 2024; Zaraś-Januszkiewicz et al., 2014, 2020), the comprehensive understanding of its entire phenological cycle and the validation of the BBCH-scale is still limited.

The aim of this study is to provide a detailed characterization of the full phenological cycle of *Ailanthus altissima* using the BBCH-scale coding system. To our knowledge, this is the first study that applies the complete BBCH-scale to this species, with phenological stages monitored separately for male and females. Besides, a novel aspect of this study was the two-year monitoring under relatively consistent meteorological conditions, which enhanced the accuracy and reliability of the phenological description. This interannual homogeneity minimizes the potential influence of climatic fluctuations, ensuring that phenological patterns reflect intrinsic biological development. This standardized approach will enable reliable comparisons across time and regions, providing a solid scientific foundation for optimizing the timing of control measures. By improving our understanding of the species' growth dynamics and reproductive behavior, this study may contribute valuable tools for developing more effective, evidence-based management strategies against one of Europe's most aggressive invasive plants.

2. Material and methods

2.1. Description of the study area

The study was conducted on a population of *Ailanthus altissima* located in Cuenca (central-eastern Spain; 40.0766, −2.2014). The area presents sandy loam soil and is located at 901 m above sea level, near a secondary road and a river, surrounded by agricultural land (mainly cereal crops) and dense Mediterranean pine forests; which according to Cabra-Rivas et al. (2016) are key aspects for the settlement of the species. Biogeographically, the area is situated within the Mediterranean Region (Western Mediterranean Subregion), specifically in the Central Iberian Mediterranean Province (Castellean Subprovince) (Rivas-Martínez et al., 2017b). Moreover, the region is placed in the supra-Mediterranean belt and presents an upper dry ombroclimate (Rivas-Martínez et al., 2017a). The climate is classified as Mediterranean-continental, characterized by cold winters and hot, dry summers with significant thermal fluctuations. Average temperatures range between 3.1°C in January and 21.9°C in July (AEMET, 2012), while annual precipitation and average temperature are around 500 mm and 11.7°C, respectively. To ensure the selection of study years with relatively uniform meteorological conditions, weather data were obtained from a Vantage Pro 2 station (Davis Instruments Corp., CA, USA) situated at 0.5 km from the study area and belonging to the Regional Institute of Agri-Food and Forestry Research and Development of Castilla-La Mancha (IRIAF). Data collected included maximum, minimum and average temperatures (°C), precipitation (mm), relative humidity (%) and insolation (hours), considering months and years. Similarly, long-term climatic data (reference period: 1991–2020) were obtained from the Cuenca weather station, operated by the Spanish State Meteorological Agency (AEMET). Statistical differences in meteorological variables between the study years and relative to the reference period were assessed using a one-way ANOVA followed by a post-hoc Tukey HSD test ($p < 0.05$), performed in SPSS Statistics Version 25 (IBM Corp., NY, USA).

2.2. Experimental design

Prior to the experiment, a total of 20 adult individuals (10 male and 10 female; N = 20) were selected for phenological monitoring. Although this number may appear limited, such sample sizes are common and well-supported in phenological studies of tree species, particularly when applying the BBCH scale (Fournier and Alfredo, 1974; Mabusela et al., 2024; Rojo and Pérez-Badia, 2014). Species identification was straightforward, as *A. altissima* is easily recognized by its compound leaves and smooth grey bark. Sex differentiation was based on the presence of persistent samaras observed in female trees during winter, a method that allowed reliable identification before the start of the study. Although no empirical measurements (e.g., diameter or health indices) were taken, all selected trees were of similar size, visibly health and grew under similar conditions, minimizing potential variability unrelated to sex or phenological stage. Despite suggestions that *A. altissima* is a monoecious tree or exhibits bisexual flowers, the evidence is lacking (Kowarik and Säumel, 2007). Consistently, the microscopic observations (Fig. 1) revealed that female flowers contain stamens and pistils (hermaphrodite flowers) but lack pollen, contrary to male flowers, as also reported by Nooteboom (1962). Identification was considered with an estimated spatial separation of approximately 2 m between trees to minimize possible interactions and ensuring independent individual and sexual analysis. Taking advantage of the similar meteorological conditions observed in 2023 and 2024 (Table 1), data collection was monitored weekly. This stability in environmental factors enhanced the reliability of detecting progressive variations in morphological aspects, ensuring that changes are primarily related to normal biological development rather than being affected by interannual variability. This *in situ* monitoring was carried out by combining direct and indirect

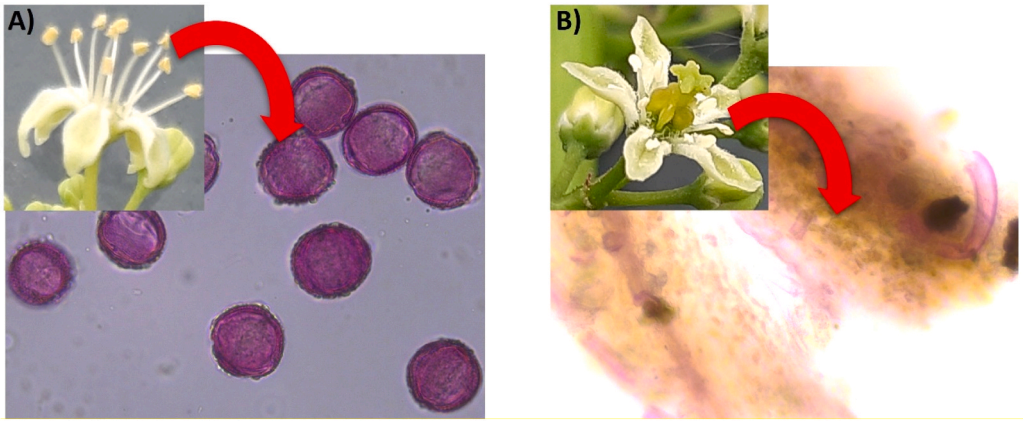

Fig. 1. Optical microscope view (40x) of A. altissima: (A) Male flower with pollen grains; (B) Female flower and anther, lacking pollen.

Table 1
Monthly means ± SD of climatic variables in the study area for 2023, 2024 and the reference period (1991–2020).

Month	Year	T_{mean} (°C)	T_{min} (°C)	T_{max} (°C)	Prec. (mm)	Accum. Prec. (mm)	RH (%)	Insolation (h)
January	**2023**	2.79 ± 2.7a*	−2.99 ± 3.5a*	9.76 ± 3.1a	1.45 ± 4.9	45.00	65.23 ± 14.1a*	5.95 ± 3.0b
	2024	5.60 ± 3.2b	0.19 ± 4.5b	12.34 ± 5.1b*	2.57 ± 6.5	79.80	77.26 ± 12.1b	4.12 ± 3.4a
	1991–2020	**5.12 ± 2.7**	**−0.01 ± 3.5**	**10.24 ± 3.8**	**1.21 ± 3.1**	**37.54 ± 3.2**	**72.47 ± 14.1**	**4.73 ± 3.2**
February	**2023**	2.88 ± 2.7a*	−4.73 ± 2.8a*	12.21 ± 4.4	0.25 ± 0.8	7.00	55.14 ± 13.2a*	6.89 ± 2.6
	2024	6.60 ± 2.0b	0.28 ± 3.3b	14.34 ± 3.8*	1.99 ± 5.9	57.80	66.28 ± 12.9b	5.40 ± 3.3
	1991–2020	**6.13 ± 3.1**	**0.37 ± 3.4**	**11.89 ± 4.6**	**1.27 ± 3.4**	**35.94 ± 3.4**	**65.15 ± 15.2**	**5.85 ± 3.5**
March	**2023**	8.52 ± 4.2	−0.48 ± 4.7a*	17.40 ± 5.0	0.33 ± 0.8a	10.20	51.03 ± 13.5a*	7.90 ± 3.0b
	2024	7.99 ± 3.5	1.60 ± 2.9b	15.10 ± 6.0	5.23 ± 9.0b*	162.00	68.03 ± 16.0b*	5.32 ± 3.9a
	1991–2020	**9.10 ± 3.2**	**2.93 ± 3.0**	**15.27 ± 4.9**	**1.53 ± 4.0**	**47.28 ± 4.1**	**59.71 ± 15.2**	**6.51 ± 3.7**
April	**2023**	12.60 ± 2.9	1.27 ± 3.2*	22.37 ± 3.8*	0.13 ± 0.7	4.00	36.13 ± 8.0a*	9.51 ± 1.6*
	2024	11.02 ± 3.1	2.67 ± 3.0*	20.20 ± 4.2*	0.18 ± 0.5	5.40	49.97 ± 13.3b*	8.02 ± 2.5
	1991–2020	**11.31 ± 3.5**	**5.18 ± 3.2**	**17.44 ± 5.0**	**2.00 ± 4.7**	**59.94 ± 4.7**	**58.55 ± 15.4**	**7.28 ± 3.8**
May	**2023**	14.05 ± 2.1	5.04 ± 3.5*	22.38 ± 3.0	1.35 ± 3.0	41.80	45.65 ± 18.4	7.00 ± 2.7
	2024	14.86 ± 4.0	5.28 ± 3.4*	23.82 ± 5.1	0.41 ± 1.4	12.80	43.00 ± 8.6*	7.54 ± 2.2
	1991–2020	**15.48 ± 3.8**	**8.89 ± 3.4**	**22.06 ± 5.2**	**1.57 ± 4.1**	**48.72 ± 4.1**	**52.90 ± 15.2**	**8.15 ± 3.9**
June	**2023**	19.51 ± 3.4	12.06 ± 2.4	27.31 ± 4.6	2.21 ± 5.6	66.40	55.63 ± 14.1b*	6.31 ± 3.1*
	2024	19.46 ± 2.7	10.46 ± 2.9*	28.08 ± 3.9	1.39 ± 3.3	41.80	44.33 ± 13.7a	7.39 ± 2.6*
	1991–2020	**20.67 ± 3.9**	**13.38 ± 2.9**	**27.95 ± 4.9**	**1.13 ± 4.5**	**33.92 ± 4.5**	**44.58 ± 13.2**	**10.03 ± 3.4**
July	**2023**	24.24 ± 2.3	13.17 ± 3.2*	33.78 ± 2.4*	0.74 ± 3.7	23.00	35.35 ± 9.3b	9.23 ± 0.9*
	2024	24.35 ± 2.0	13.38 ± 2.5*	34.43 ± 2.8*	0.51 ± 2.5	15.80	30.58 ± 7.7a*	9.21 ± 0.7
	1991–2020	**24.16 ± 2.9**	**16.38 ± 2.7**	**31.95 ± 3.3**	**0.37 ± 3.5**	**11.55 ± 3.5**	**37.88 ± 9.4**	**11.24 ± 2.2**
August	**2023**	23.39 ± 3.1	11.93 ± 3.0a*	33.76 ± 4.2*	0.00 ± 0.0	0.00	32.00 ± 5.7a*	9.79 ± 1.6
	2024	24.00 ± 2.1	13.92 ± 2.0b*	34.42 ± 2.7*	0.83 ± 2.22	25.80	37.39 ± 14.2b	8.95 ± 1.7*
	1991–2020	**23.91 ± 2.8**	**16.35 ± 3.2**	**31.46 ± 3.5**	**0.68 ± 3.7**	**21.18 ± 3.7**	**41.93 ± 10.7**	**10.41 ± 2.2**
September	**2023**	17.92 ± 2.9	10.70 ± 4.2b	26.13 ± 3.5	2.23 ± 7.8	67.00	56.20 ± 10.1b	7.48 ± 2.4
	2024	16.86 ± 2.7*	8.55 ± 4.5a*	25.81 ± 3.2	0.73 ± 3.0	21.80	49.30 ± 15.5a	7.25 ± 2.9
	1991–2020	**19.06 ± 3.3**	**12.26 ± 3.3**	**25.85 ± 4.4**	**0.73 ± 1.9**	**41.18 ± 4.6**	**52.88 ± 13.2**	**8.00 ± 3.0**
October	**2023**	13.93 ± 3.0	7.17 ± 3.0	21.91 ± 6.7	2.10 ± 5.7a	65.20	61.16 ± 18.9	5.51 ± 3.9
	2024	13.30 ± 2.4	7.56 ± 3.3	20.10 ± 3.8	4.48 ± 8.6b	139.00	68.19 ± 12.1	5.15 ± 3.2
	1991–2020	**14.01 ± 3.4**	**8.16 ± 3.6**	**19.87 ± 4.8**	**1.87 ± 4.4**	**57.98 ± 4.4**	**65.03 ± 15.2**	**6.11 ± 3.5**
November	**2023**	8.16 ± 2.7	2.87 ± 4.2	14.94 ± 3.0	1.20 ± 2.7	36.00	74.47 ± 12.6	5.04 ± 3.3
	2024	8.95 ± 2.9	3.24 ± 3.4	16.38 ± 2.7*	0.77 ± 3.3	23.00	73.60 ± 5.8	5.50 ± 2.6
	1991–2020	**8.55 ± 3.2**	**3.41 ± 3.7**	**13.68 ± 4.3**	**1.68 ± 4.0**	**50.39 ± 4.0**	**72.30 ± 13.6**	**4.83 ± 3.3**
December	**2023**	3.97 ± 2.7*	−2.26 ± 3.7*	12.18 ± 2.5	1.06 ± 3.4	32.80	71.32 ± 11.3	5.28 ± 2.7
	2024	3.64 ± 2.4*	−2.73 ± 2.8*	12.03 ± 3.7	0.05 ± 0.2	1.60	67.97 ± 8.3*	6.04 ± 2.4*
	1991–2020	**5.79 ± 2.8**	**0.73 ± 3.2**	**10.86 ± 3.7**	**1.60 ± 4.4**	**49.56 ± 4.4**	**74.28 ± 12.6**	**4.39 ± 3.1**
ANNUAL	**2023**	**12.72 ± 7.8**	**4.51 ± 7.1***	**21.19 ± 8.8**	**1.09 ± 4.0**	**398.40**	**53.24 ± 18.5a***	**7.15 ± 3.1**
	2024	**13.07 ± 7.3**	**5.37 ± 6.2***	**21.44 ± 8.6***	**1.60 ± 5.0**	**586.60**	**56.29 ± 19.2b**	**6.66 ± 3.1**
	1991–2020	**13.60 ± 7.5**	**7.22 ± 6.7**	**20.01 ± 8.8**	**1.36 ± 4.1**	**495.28 ± 12.5**	**57.89 ± 18.2**	**6.96 ± 3.9**

Different letters mean significant differences between the study years (2023 & 2024; Tukey's test $p < 0.05$). *: denotes significant differences in comparison to the reference period (1991–2020; Tukey's test $p < 0.05$). Climatic variables include mean, maximum and minimum temperatures (°C); daily and accumulated precipitation (mm); relative humidity (%); and insolation (hours)

observations, including the use of binoculars and photographic documentation to graphically record the entire biological cycle.

2.3. BBCH-scale assessment

Following the BBCH-scale guidelines established by Finn et al. (2007) for woody species, eight of ten principal stages were considered for *A. altissima* (omitting stages 2 and 4, not applicable to this species) and grouped into four categories by sex. The first category (I) corresponds to vegetative growth: including bud development (BBCH 0), leaf development (BBCH 1) and shoot elongation (BBCH 3). The second category (II) refers to reproductive growth, starting with inflorescence

emergence (BBCH 5) and flowering (BBCH 6). The third category (III) is related to the development and maturation of fruits and seeds (BBCH 7 and 8), only for female individuals. The last category (IV) corresponds to the onset of senescence (BBCH 9), existing in both sexes. Since, BBCH 8 and BBCH 0 represent analogous developmental stages occurring in consecutive years, only a single data record was collected for these phases. The estimation of each phenological stage was carried out by assigning a percentage value to each phenophase in every observation for category. This approach allowed for accurate and continuous assessment of phenological development using the linear interpolation method (Weighted Plant Development), similar to that reported by Cornelius et al. (2011) and Rojo and Pérez-Badia (2014). The method categorizes phenological stages grouped on a scale from 0 to 9, effectively describing the seasonal course of phenological phases of *A. altissima* from dormancy to plant senescence.

2.4. Data processing and statistical analysis

The daily mean of meteorological variables—including maximum, minimum, and average temperature, precipitation, humidity and insolation—were analysed in relation to the sex of *Ailanthus altissima* specimens. Additionally, total accumulated precipitation was calculated and the number of days exceeding specific climatic thresholds was evaluated. Since certain phenological stages (BBCH 0 and 8) span multiple years, meteorological data from January 2023 to December 2024 were used. Although phenological data were collected across two consecutive growing seasons, preliminary analysis indicated minimal interannual variation in the onset and duration of phenophases. Therefore, data from both years were integrated to generate a more robust and representative phenological model for the species. This year-to-year consistency supports the descriptive and standardizing objective of the study, rather than comparative analyses between dry and wet years. Data analysis and figure generation were performed using R version 4.4.2 (R Core Team, 2025). To assess statistical differences between sexes, a one-way ANOVA followed by Tukey's HSD post-hoc test was conducted using SPSS Statistics version 25 (IBM Corp., NY, USA). Likewise, bilateral Pearson's correlation analysis was used to determine the relationship between climatic conditions and the duration of each phenophase. The observed associations between *A. altissima* phenophases and key meteorological variables (temperature and precipitation) led to the development of a detailed phenological calendar.

3. Results

According to the BBCH-scale, a total of 41 secondary stages were identified across the 8 main stages in *A. altissima* (Fig. 2 & Table 2), showing considerable overlap in the duration of some phases (Fig. 3). Overall, several meteorological parameters, particularly extreme temperatures (both minimum and maximum), exhibited significant long-term differences (Table 1). During the study period, temperatures ranged from a minimum of −10.4°C on March 2 to a maximum of 39.9°C on August 9, 2023. Notably, July and August were the warmest months, with average temperatures of 24.3°C and 23.7°C, and average maximum temperatures exceeding 34°C, significantly higher than the 1991–2020 reference values. December was the coldest month, with an average temperature of 3.7°C, also significantly lower than the historical average. Precipitation was highly variable, with peaks in March 2024 and, particularly, in October 2024, when 139 mm were recorded, considerably above typical levels. Conversely, April was the driest month in both years, with precipitation consistently below the reference period. February and March 2023 were also among the months with the lowest precipitation. Relative humidity and insolation exhibited more subtle trends; however, notable deviations were observed in certain months when compared to the reference period. Importantly, meteorological patterns between both years were broadly consistent, with no substantial asynchrony in key climatic variables such as temperature, rainfall timing, or solar radiation. Consequently, the phenological stages of *A. altissima* showed year-to-year consistency, with only minor variation in the timing and duration of developmental phases. This temporal stability strengthens the decision to integrate the data from both years and supports the reliability of the phenological description developed using the BBCH-scale.

The phenological cycle began with dormancy and bud development (**BBCH 0**). Dormancy occurred earlier in males, from the end of November to the first half of April. In contrast, females began the cycle in mid-December, extending until the end of April, lasting approximately 136 days—slightly longer than in males (Table 3). This phase started with dormancy, followed by the appearance of small buds covered in brown scales at the nodes of the branches in March/April. As the season progressed, these buds swelled, and as the scales separated, leaf buds emerged. At this stage, the tips of the leaves became visible, eventually leading to the full development of leaves with green tips. During this phase, meteorological conditions included daily minimum temperatures below 0°C, accumulated precipitation of 196 mm, an average temperature of approximately 6–7°C, relative humidity of 70 %, and around 5 h of insolation. Although females showed higher temperatures and sunlight exposure compared to male individuals, the differences were minor.

The leaf development phase (**BBCH 1**) began in mid-April and ended in early May, first appearing in male specimens. It involved the growth and expansion of leaves, lasting about 36 days in males and 26 days in females, with significant differences. The leaves emerged progressively, starting with the first leaves, then the unfolding of the first young leaf, until they reached full size. During this period, average temperatures gradually increased to 13°C, with daily highs of 23°C and lows around 3°C. Precipitation was minimal, with only 4 mm accumulated, and approximately 8 h of daily sunshine were recorded, with male individuals exhibiting slightly higher sunlight exposure than females.

The shoot elongation phase (**BBCH 3**) started in mid-May and first appeared in male specimens. During this process, the stem progressively elongated from its beginning until it reached nearly its final length. This phase ended at the end of June, with an average duration of 36 days in both sexes. Differences were observed in the coloration of the leaves: the basal leaflets showed darker tones, while the upper ones developed greenish tones with reddish tints. Meteorological conditions during this phase were favourable, with 65 mm of accumulated precipitation, a slight increase in temperatures, and relative humidity close to 50 %.

Reproductive growth began with the emergence of inflorescences (**BBCH 5**) around mid-May, marking the onset of reproductive development. Initially protected by reddish-brown scales, the buds began to swell, revealing the floral primordia. As development progressed, the buds expanded, and the flowers began to open, reaching full bloom in early June. The average temperature was 16°C, with approximately six hours of daily sunlight, while relative humidity remained above 50 %. This stage lasted differently for males (23 days) and females (21 days), with more intense rainfall by the end of the phase, accumulating 39.4 mm and 42.5 mm, respectively.

Subsequently, flowering (**BBCH 6**) began in early June and continued until late June, lasting an average of 17 days in both sexes, with males starting approximately one day earlier (Fig. 3). Flowering progressed through distinct stages in both male and female flowers, starting when the first flowers opened and continuing until most were in full bloom. The phase ended with the petals falling or drying in males and fading in females. Environmental conditions included an average temperature of 20°C, with daily peaks reaching up to 29°C. Relative humidity averaged around 45 %, accompanied by approximately seven hours of sunlight per day.

The fruit and seed phases began with fruit development (**BBCH 7**) in female specimens at the end of June, lasting until mid-July, with an average duration of 24 days. During this phase, the fruits progressed through several stages: from the initial formation of barely visible ovaries, followed by the gradual increase in size, and ending with the

Fig. 2. Phenological growth stages of *Ailanthus altissima* according to the extended BBCH scale.

Table 2
Phenological description for Ailanthus altissima (Mill.) Swingle using the extended BBCH scale.

BBCH Code	Description
Principal growth stage 0: Sprouting/Bud development	
00	Dormancy: leaf and flower buds are closed and covered by greyish-brown bud scales
01	Beginning of bud swelling: bud appear prominent over bark
03	End of bud swelling: brown scales covering the bud scales completely separated
07	Beginning of bud burst: leaf tips start to become visible
09	End of bud burst: green leaf tips are clearly visible
Principal growth stage 1: Leaf development	
10	First leaves separated: green leaf tips around 10 mm above the bud scales. First leaf is separated
11	First young leaf unfolded: first leaf unfolds and spreads away from the shoot
15	More leaves unfolded: without reaching its full size and petioles become visible
19	Leaf expansion complete: leaves attain full size
Principal growth stage 3: Steam elongation	
30	Beginning of stem elongation: axes of developing shoots visible
31	Stem about 10 % of final length: basal leaflets darker green and upper leaflets green with reddish.
33	Shoots about 30 % of final length: basal leaflets darker green and upper leaflets green with reddish.
35	Shoots about 50 % of final length: basal leaflets darker green and upper leaflets green with reddish.
37	Shoots about 70 % of final length: basal leaflets darker green and upper leaflets green with reddish.
39	Shoots about 90 % or more of final length: basal and upper leaflets dark green
Principal growth stage 5: Inflorescence emergence	
50	Inflorescence buds dormant: bud covered in reddish-brown scales with no signs of growth
51	Inflorescence buds swelling: buds covered with light brown scales that begin to separate
53	Inflorescence buds burst: bud scales folded back, first floral primordia just visible in axils of bud scales
55	Swollen flower buds: flower buds visibly separated, greenish downy outer sepals closed, elongation of branchlet starts
57	Flower buds 70 % of final length: individual flower pedicels elongated, light green outer sepals closed, flowers differentiated and closed.
59	End of flower bud extension: 90 % of elongated panicle flower pedicels, light green outer sepals and inner sepals slightly visible between them.
Principal growth stage 6: Flowering (male flower)	
60	First flowers open: petals begin to separate
61	Beginning of flowering: 10 % of flowers open
63	Early flowering: 30 % of flowers open
65	Full flowering: more than 50 % of flowers in umbel opened
67	Beginning of flower fading: majority of petals dried or fallen
69	End of flowering: all petals have fallen off or dried out and the branchlet is clearly visible
Principal growth stage 6: Flowering (female flower)	
60	First flowers open: tepals start separating, stigma fully exposed
61	Beginning of flowering: 10 % of flowers open
63	Early flowering: 30 % of flowers open, carpels have a light yellowish-green colour
65	Full flowering: more than 50 % of flowers in umbel opened, carpels have a light brown-green colour
67	Beginning of flower fading: stigma receptivity ceased, fading of stigma started, carpels have a light brown colour
69	End of flowering: most of the female flowers start fading, completion of female phase; fruit set started, carpels have a reddish-brown colour
Principal growth stage 7: Fruit development	
70	Fruit set: no ovary growth visible
71	Initial ovary growth: the style is still present on the ovary covered with a fine downs and surrounded by dried sepals.
72	Fruits is about 20 % of final size, already showing characteristic form in samara
75	Fruits at 50 % of final size: seed enlargement and the outline of the seeds are clearly visible. The colour of the fruit can be from light yellow to brown.
79	Fruits with 90 % or more of the final size: the samara turns greenish yellow or reddish brown; seed hardening begins and seed development is completed.
Principal growth stage 8: Fruit maturation	
81	Beginning of fruit ripening: slightly lighter colour changes of the samara
85	Advanced ripening: the fruit is still firm and the samara turns light red-yellowish
87	Fruit ripe: fruit colour becomes more intense, colour of seed coat starts turning brown, seed maturation completed, seeds turn light yellowish-brown in colour
89	Fully ripe fruit: the seed coat turns brown, samara ripening is complete, the seed is dark-brown
Principal growth stage 9: Beginning of dormancy	
91	Shoots and leaves cease growth and foliage still dark green.
92	Beginning of leaf discoloration from dark green to brown-green.
93	Beginning of leaf fall
95	50 % of leaves fallen; majority of leaves greenish yellow and yellowish-brown.
97	End of leaf fall; in female specimens seeds continue on the tree.

formation of samaras. This occurred under an average temperature of 24°C, limited precipitation (19 mm), and low humidity (34 %). The cycle continued with the ripening of the samaras (fruits) (**BBCH 8**) in mid-July, highlighted by a change in coloration. This shift gradually became uniform until the samaras reached their final colour and optimal texture for dispersal, culminating in full maturation. In this two-year study, the onset of maturation was observed in mid-July, though its completion extended into August of the following year, indicating the presence of samaras from previous cycles.

Finally, the cycle concluded with the senescence phase (**BBCH 9**), observed in mid-September, starting earlier in male specimens. This phase was significantly different between males (64 days) and females (73 days), characterized by a gradual decrease in temperature, with notable differences between male individuals, which were somewhat higher than those of females due to an earlier start of this phenophase, as well as variations in precipitation and photoperiod. This stage was characterized by a progressive slowdown in shoot elongation, followed by a transition in leaf colour from dark green to greenish-brown tones, eventually culminating in complete leaf fall by mid-November. This marked the end of the phenological cycle and the beginning of the dormancy period.

4. Discussion

This study presents the first comprehensive application of the BBCH-scale to *Ailanthus altissima* and offers valuable preliminary insights into potential sex-based phenological differences. Despite being conducted at a single site and over two calendar years, this work lays a solid foundation for future research. The main stages detected for *Ailanthus altissima*, as in other evergreen tree species, underscore the versatility and wide applicability of the BBCH-scale in phenological analyses of species with diverse biological characteristics, further confirming its effectiveness in monitoring invasive species (Fridley, 2012; Funk et al., 2016; Maan et al., 2020). The omission of stages 2 and 4 is justified because the growth of the main stem after germination is less relevant, while stage 4 is associated with herbaceous species with harvestable parts (Finn et al., 2007; Meier, 2001). In addition, the number of secondary stages observed in *A. altissima* is similar to that of other perennial tree species, such as *Morus sp.* (39 secondary stages; Sánchez-Salcedo et al., 2017), but differs from others, such as *Sapium sebiferum* (24 secondary stages; Jaryan et al., 2014) or *Prunus dulcis* (49 secondary stages; Sakar et al., 2019), among others. This knowledge is crucial for developing management strategies to limit its spread in invaded areas, as no control method (herbicides or biologicals) has been proven to be completely effective. Effective management of this invasive tree requires integrated strategies combining trunk-injected herbicides with potential new active ingredients and biological control agents, while assessing their efficacy and safety for native flora to ultimately achieve eradication (Soler and Izquierdo, 2024). Since previous studies indicate that interventions

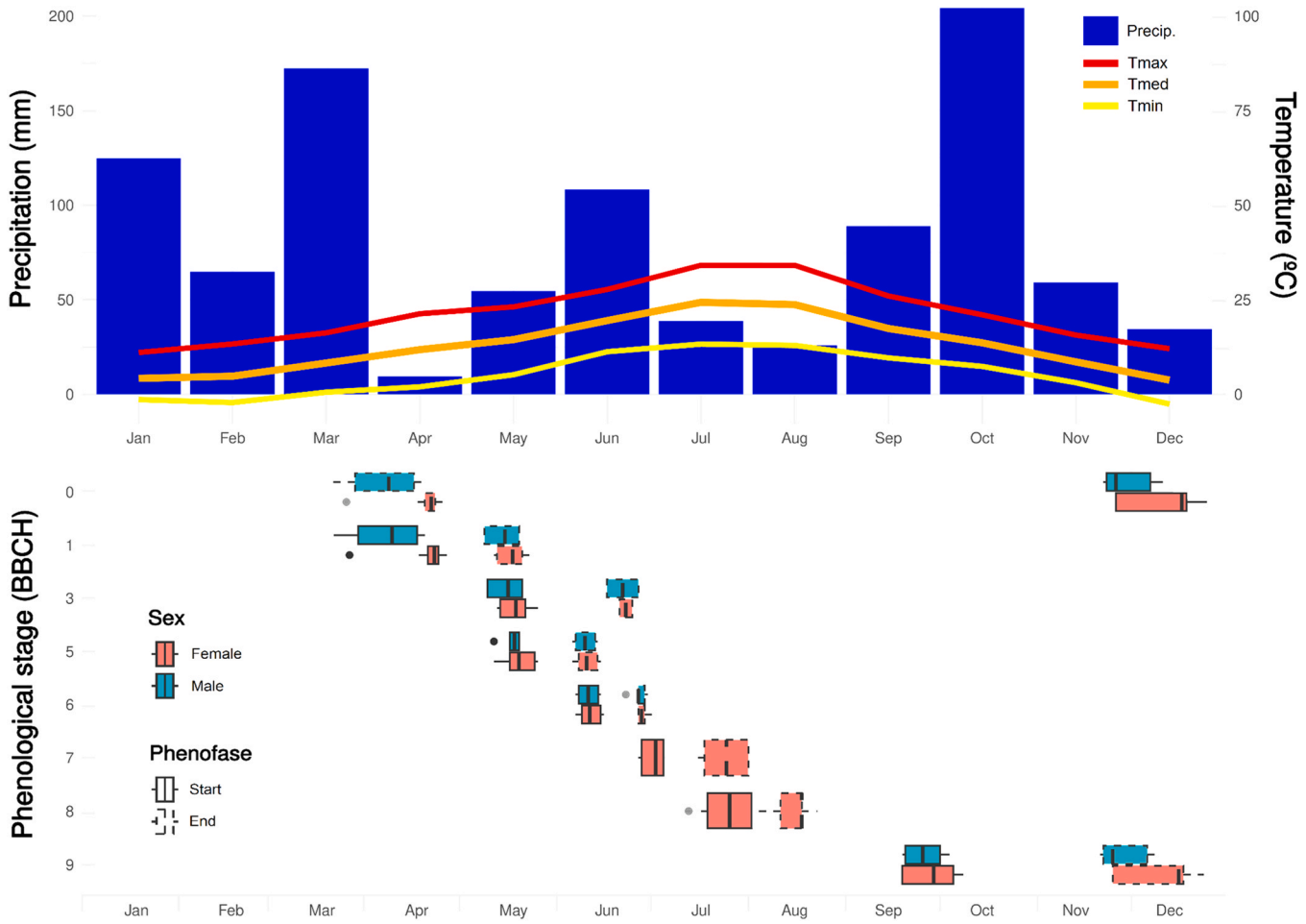

Fig. 3. Meteorological conditions and phenological calendar during the study period (2023–2024): (top) Mean, maximum and minimum temperatures (°C) and precipitation (mm); (bottom) Timing of the main phenological stages of Ailanthus altissima.

during pre-flowering or early reproductive stages are most effective in preventing seed dispersal and limiting the spread of other invasive species (Jaryan et al., 2014; Maan et al., 2020), identifying critical stages in *A. altissima* would help determine the optimal timing for control treatments. In this context, the BBCH-scale aids in estimating phenological development, allowing the correlation of *A. altissima* phases with flowering and pollen dispersal, which helps predict peak pollen scenarios. This is particularly valuable for managing the species and addressing public health concerns, especially in urban areas where this plant is widespread and associated with allergic reactions (Werchan et al., 2024). Moreover, correlating phenological observations in situ (developmental phases) and climatic parameters with remote sensing techniques (spectral information) offers new opportunities for large-scale monitoring. Additionally, citizen science platforms such as iNaturalist, where projects focused on invasive species like *Ailanthus altissima* already exist (Kheloufi, 2019) and can provide valuable photographic records for inventory and phenological studies. Recent studies demonstrate that non-professional observers can significantly contribute to flowering biology research across large spatial scales (Aavik et al., 2025; Puchałka et al., 2022). When combined with rigorous data analysis and complementary technologies, these participatory approaches can help detect early invasion hotspots and assess the effectiveness of management strategies, even in remote or under-surveyed areas.

Understanding the influence of key factors on the distribution of invasive species is also crucial for effective management, where climate is the primary determinant of tree species distribution. Among these factors, average annual temperature and thermal conditions play a significant role (Booth, 2016; Körner, 2021), along with water availability. Thermal fluctuations are also a critical factor, as heat promotes the development of vegetative phases, while cold induces dormancy, particularly in deciduous trees (Vitasse et al., 2014). In Mediterranean climates, *A. altissima* thrives at mean daily temperatures between 15 and 20°C, which promote the development of vegetative structures such as stems and secondary roots (Kowarik and Säumel, 2007). Conversely, daily mean temperatures below 10°C hinder its expansion, particularly during juvenile stages (Kowarik and Säumel, 2007; Von der Lippe et al., 2005). Although Filippou et al., (2014) observed drought tolerance due to its deep root system, Walker et al., (2017) detected limited expansion in harsh arid climates. Furthermore, since *A. altissima* is a heliophilous species, its growth is strongly influenced by solar radiation (Kowarik and Säumel, 2007). In our study area, average daily temperatures consistently exceeded 10°C from April to October, demonstrating optimal conditions for its development. Despite minimum temperatures dropped to −10.4°C, adult individuals demonstrated strong resilience. On the contrary, temperatures below −15°C could lead to setbacks, potentially affecting the tree development in subsequent years (Kuhn, 1957; Scheerer, 1956). Rainfall variability is mitigated by proximity to water sources and seasonal rainfall events, particularly in autumn, which promotes soil recharge, essential for the storage of reserves and the initiation of spring bud break. During this study period, an average of 7 h of sunshine per day was recorded, which is crucial for enhancing physiological processes and biomass production throughout the vegetative cycle. Importantly, both years of observation exhibited similar

Table 3
Mean ±SD of climatic variables recorded in the study area and the period 2023–2024 for each phenological stage (BBCH) of Ailanthus altissima, categorized by phenophase (BBCH) and sex.

Phenophase	Sex	Duration (days)	T_{mean} (°C)	T_{min} (°C)	T_{max} (°C)	Prec. (mm)	Accum. Prec. (mm)	RH (%)	Insolation (h)
0	**Female**	139.20 ± 12.7	6.99 ± 0.1a	0.52 ± 0.1a$^{(-)}$	14.71 ± 0.2a$^{(-)}$	0.10 ± 0.1	196.83 ± 145.08	67.62 ± 0.9a	5.45 ± 0.1a
	Male	133.70 ± 6.9	6.23 ± 0.2b$^{(+)}$	0.09 ± 0.2b$^{(+)}$	13.75 ± 0.2b$^{(+)}$	0.15 ± 0.1	196.37 ± 145.16	70.07 ± 0.5b	5.10 ± 0.1b
	MEAN	**136.45 ± 10.3**	**6.61 ± 0.4**	**0.31 ± 0.3**	**14.23 ± 0.5**	**0.13 ± 0.1**	**196.60 ± 145.12**	**68.85 ± 1.5**	**5.28 ± 0.2**
1	**Female**	26.10 ± 7.5a	13.66 ± 1.7$^{(-)}$	3.71 ± 0.6a$^{(-)}$	22.79 ± 2.3$^{(-)}$	2.91 ± 0.6a	6.56 ± 5.56a	40.37 ± 6.6$^{(+)}$	8.05 ± 1.0
	Male	36.30 ± 11.4b	13.30 ± 1.6$^{(-)}$	3.18 ± 0.7b$^{(-)}$	22.67 ± 2.1$^{(-)}$	2.50 ± 0.3b	11.74 ± 15.05b	41.01 ± 6.8$^{(+)}$	8.45 ± 0.9$^{(-)}$
	MEAN	**31.20 ± 10.8**	**13.48 ± 1.6$^{(-)}$**	**3.44 ± 0.7$^{(-)}$**	**22.73 ± 2.2$^{(-)}$**	**2.70 ± 0.5**	**9.15 ± 10.31**	**40.69 ± 6.6$^{(+)}$**	**8.25 ± 0.9**
3	**Female**	35.30 ± 7.1	17.51 ± 1.2$^{(-)}$	9.25 ± 0.3a	25.75 ± 1.9$^{(-)}$	1.60 ± 0.3$^{(+)}$	64.65 ± 43.45	49.94 ± 7.9$^{(+)}$	6.71 ± 1.0$^{(-)}$
	Male	37.25 ± 0.9	16.84 ± 1.8	8.46 ± 0.6b	25.14 ± 2.7	1.93 ± 0.7	65.8 ± 37.55	49.72 ± 7.7	6.69 ± 1.1
	MEAN	**36.28 ± 5.1**	**17.17 ± 1.5$^{(-)}$**	**8.85 ± 0.6**	**25.44 ± 2.3$^{(-)}$**	**1.76 ± 0.5**	**65.23 ± 40.50**	**49.83 ± 7.7$^{(+)}$**	**6.70 ± 1.1$^{(-)}$**
5	**Female**	21.00 ± 4.3	16.34 ± 1.9	8.80 ± 0.9a$^{(-)}$	24.38 ± 2.8	1.95 ± 0.5$^{(+)}$	42.46 ± 21.55	54.41 ± 11.5$^{(-)}$	6.07 ± 1.5$^{(+)}$
	Male	22.85 ± 1.8	16.02 ± 1.8$^{(+)}$	8.18 ± 0.5b	24.15 ± 2.6$^{(+)}$	1.91 ± 05$^{(+)}$	39.39 ± 16.65	52.23 ± 8.9$^{(-)}$	6.20 ± 1.3$^{(+)}$
	MEAN	**21.93 ± 3.4**	**16.18 ± 1.8$^{(+)}$**	**8.49 ± 0.8$^{(-)}$**	**24.26 ± 2.7$^{(+)}$**	**1.93 ± 0.5$^{(+)}$**	**40.93 ± 19.10$^{(+)}$**	**53.32 ± 10.2$^{(-)}$**	**6.13 ± 1.4$^{(+)}$**
6	**Female**	16.70 ± 4.8	20.46 ± 0.4a$^{(+)}$	11.11 ± 1.4$^{(+)}$	29.20 ± 0.4a$^{(-)}$	0.68 ± 0.3$^{(-)}$	22.92 ± 20.12	44.86 ± 6.3$^{(+)}$	7.74 ± 0.7$^{(-)}$
	Male	16.50 ± 2.9	20.09 ± 0.5b$^{(+)}$	11.12 ± 1.5$^{(+)}$	28.68 ± 0.8b$^{(-)}$	0.65 ± 0.4$^{(-)}$	32.81 ± 19.56	46.79 ± 7.0$^{(+)}$	7.42 ± 0.9$^{(-)}$
	MEAN	**16.60 ± 4.0**	**20.27 ± 0.5$^{(+)}$**	**11.11 ± 1.4$^{(+)}$**	**28.94 ± 0.6$^{(-)}$**	**0.66 ± 0.3$^{(-)}$**	**27.87 ± 19.84$^{(-)}$**	**45.82 ± 6.7$^{(+)}$**	**7.58 ± 0.8$^{(-)}$**
7	**Female**	22.95 ± 4.2	24.41 ± 0.4$^{(+)}$	13.60 ± 0.2	34.20 ± 0.7$^{(+)}$	0.78 ± 0.1	19 ± 4,1	34.51 ± 4.5$^{(-)}$	9.09 ± 0.2$^{(+)}$
	Male	n.d.	n.d.	n.d.	n.d.	n.d.	n.d.	n.d.	n.d.
	MEAN	**n.d.**	**n.d.**	**n.d.**	**n.d.**	**n.d.**	**n.d.**	**n.d.**	**n.d.**
8	**Female**	386.20 ± 11.8	13.73 ± 0.4$^{(+)}$	5.75 ± 0.2$^{(+)}$	22.15 ± 0.5$^{(+)}$	0.56 ± 0.5	491.75 ± 177.8	54.72 ± 0.8$^{(-)}$	6.83 ± 0.1$^{(+)}$
	Male	n.d.	n.d.	n.d.	n.d.	n.d.	n.d.	n.d.	n.d.
	MEAN	**n.d.**	**n.d.**	**n.d.**	**n.d.**	**n.d.**	**n.d.**	**n.d.**	**n.d.**
9	**Female**	73.00 ± 8.0a	10.45 ± 1.3a$^{(-)}$	4.39 ± 0.8a$^{(-)}$	17.90 ± 1.7a$^{(-)}$	1.46 ± 0.8	134.04 ± 31.45	68.28 ± 3.7	5.53 ± 0.4
	Male	64.20 ± 2.6b	11.64 ± 0.8b$^{(-)}$	5.40 ± 0.4b$^{(-)}$	19.23 ± 1.2b	1.48 ± 1.0	128.29 ± 64.33	67.25 ± 3.1	5.67 ± 0.2
	MEAN	**68.60 ± 7.4**	**11.05 ± 1.2(-)**	**4.89 ± 0.8(-)**	**18.56 ± 1.6(-)**	**1.47 ± 0.9**	**131.17 ± 47.89**	**67.76 ± 3.4**	**5.60 ± 0.3**

n.d.: not determined for male individuals. Different letters indicate significant differences between sexes. $^{(+/-)}$: indicates positive/negative significant correlation (2023 & 2024; Pearson's test, $p < 0.05$). Climatic variables include daily mean, maximum, and minimum temperatures (°C); daily and accumulated precipitation (mm); relative humidity (%); and insolation (hours)

meteorological conditions and phenological trends, supporting the year-to-year consistency of our data and reinforcing the robustness of the observed patterns. This consistency supports the further use of the BBCH scale in long-term phenological studies of invasive species.

Throughout this study, it was observed that *A. altissima* exhibits distinctive phenology compared to native species (Castro-Diez et al., 2014; Motti et al., 2021), allowing it to expand into a wide range of niches while reducing interspecific competition for resources. The vegetative dormancy begins at the end of November for males and in mid-December for females, which could be explained by its sensitivity to thermal variations. The end of phase 0 occurs in early April for males and late April for females, as temperatures and sunlight increase. This trend has also been observed in a riparian habitat of Madrid (near our study area) (Castro-Diez et al., 2014), but also in its native distribution area in China (Hu, 1979). The delay in females suggests a longer dormancy phase, which could be related to energy demands during samara production. Dormancy depends not only on environmental factors, but also on internal physiological processes, such as endodormancy, affecting growth pattern due to hormonal factors (Yang et al., 2021). During the beginning of leaf development, a slight asynchrony was observed in the growth of both sexes. Males begin to sprout earlier than females, being supported due to their greater hormonal sensitivity to gibberellins, which facilitate early sprouting and the interruption of dormancy (Ritonga et al., 2023). This previous budding, added to a longer period, allows males to accelerate the growth of their leaves, facilitating the accumulation of energy for the production of flowers and pollen (Barrett and Hough, 2013). In contrast, females exhibit a delayed onset of sprouting, possibly due to a stricter hormonal regulation that prioritizes energy accumulation before leaf development, leading to greater production of samaras. Additionally, both sexes finish this phase almost simultaneously, demonstrating how environmental factors, such as the progressive increase in solar radiation and temperature, foster a convergence in leaf development. From the third phenophase, a greater synchronization was observed between sex, with minimal differences in their start and finish time. Environmental factors such as temperature and humidity likely contributed to this uniformity by providing similar optimal conditions. Along this line, Castro-Diez et al. (2014) reported a comparable pattern of vegetative development in Madrid, where this phenophase also concluded in mid-June.

Similarly, inflorescence emergence and flowering phases showed synchronization between sex, ensuring that pollen is available at the optimal time for female flowers, thereby maximizing pollination efficiency. Furthermore, male flowers were observed to emit a distinctive odour, suggesting that this species also relies on insect pollination (entomophilous) (Thompson, 2021). Temporal alignment with the insect's activity during the warmer months improves its reproductive success, contributing to its high invasive potential. In our study area, flowering lasted approximately 17 days for both sexes, comparable to a previous study in Poland, where lasted around 14 days (Zaraś-Januszkiewicz et al., 2014). In contrast, longer flowering periods have been reported in other studies, such as in Madrid (Spain), where it extended from mid-May to late June (Castro-Diez et al., 2014); or in Germany, where Werchan et al. (2024) recorded an average duration of 29 days (June 13 to July 10). The shorter flowering period observed in this study may be attributed to moderate pre-flowering temperatures followed by a strong increase in late June (>30 °C). The fruiting phase occurred during the warmest and sunlight period, completing in approximately 23 days. These conditions appeared to play a crucial role in fruit development, while the dry environment helped minimize the incidence of moisture-related diseases, such as fungal infections.

Similarly, higher temperatures and longer photoperiods have also been identified as key factors in fruit maturation for warm-climate species like mango (*Mangifera indica*) (Hussen, 2021) and durian (*Durio zibethinus*) (Ketsa and Pangkool, 1995). Unexpectedly, the fruit maturation in *Ailanthus altissima* began in late July and extended until early August of the following year, lasting over a year. This pattern has also been observed in Madrid (Spain) where fruits remain present year-round (Castro-Diez et al., 2014), but also in its native area, where trees retain fruits during the winter and gradually disperse them in spring (Hu, 1979). This prolonged maturation allows the coexistence of fruits from consecutive cycles, ensuring a continuous supply of seeds. Furthermore, fruit ripening during periods of low competition with native species facilitates dispersal and persistence in new habitats (Gosper, 2004; Lediuk et al., 2014; Yang et al., 2022). This strategy, known as *gap filling*, is a crucial driver of invasive species' success, significantly enhancing their ability to colonize and establish in new environments. Finally, the vegetative dormancy phase exhibits notable differences between sexes. Female individuals prolong senescence to support fruiting, which requires additional time and resources, resulting in a later dormancy onset. In contrast, males enter this phase earlier, optimizing energy expenditure after completing their reproductive role and initiating dormancy sooner. These differences underscore a functional specialization in resource allocation, enhancing the competitive advantage of *A. altissima* in diverse ecosystems.

Beyond the phenological insights, understanding the potential spatial expansion of *Ailanthus altissima* is essential for anticipating future invasion risks, particularly under climate change scenarios. Several ecological niche models and GIS-based studies have projected increased habitat suitability for this species across Europe and North America, often linked to warmer temperatures and human-altered landscapes (Clark et al., 2014; de Groot et al., 2024; Motti et al., 2021). These studies suggest that *A. altissima* tends to follow broader networks and expand into low-elevation areas with mean annual temperatures above 11 °C. However, no predictive modelling efforts currently exist for the Iberian Peninsula, especially inland Mediterranean regions like our study area (highlighting a clear research gap). The phenological data provided here could serve as valuable input for future distribution models of other species, improving invasion forecasts and inform early-warning strategies in vulnerable Mediterranean landscapes. These findings are relevant for optimizing control strategies, including urban environments where the species causes allergies.

5. Conclusions

This study provides a preliminary analysis of the phenology of the invasive species *Ailanthus altissima* using the BBCH scale, identifying eight key stages that align patterns observed in other evergreen tree species. However, these insights are limited by several factors, including constrained long-term data, the lack of robust information for BBCH stages 0 and 8 and the close proximity between individuals, which hinders a long-term conclusion and the comprehensive understanding of its life cycle. Nonetheless, the findings presented here provide a valuable foundation for developing management strategies aimed at reducing ecological, economic and social impacts of *A. altissima*. In particular, identifying critical phenophases can help optimize the timing of control interventions, especially during reproductive stages. Moreover, predicting periods of peak pollen release has important implications for public health, particularly in urban environments where this species is widespread and associated with allergic reactions. In this context, developing reliable methods to differentiate male and female individuals in the field becomes increasingly relevant. Future research should aim to validate these results across diverse environments by integrating in situ phenological monitoring with remote sensing, citizen science contributions, and ecological niche models. This combined approach will enhance our ability to monitor, predict, and manage the spread of *A. altissima*. Additionally, further studies with longer time series should consider applying more advanced statistical frameworks to better capture the interaction effects between sex and interannual variability on phenological behavior. Finally, this framework may also be applicable to other invasive tree species occupying similar ecological niches, contributing to the design of more effective local eradication or containment strategies.

CRediT authorship contribution statement

Jorge Romero-Morte: Writing – review & editing, Writing – original draft, Supervision, Methodology, Investigation, Formal analysis, Data curation, Conceptualization. **Gonzalo Ortiz de Elguea-Culebras:** Writing – review & editing, Methodology, Formal analysis, Data curation, Conceptualization.

Declaration of Competing Interest

The authors declare that they have no known competing financial interests or personal relationships that could have appeared to influence the work reported in this paper.

Acknowledgments

The authors gratefully acknowledge the Complutense University of Madrid and the Regional Institute of Agri-Food and Forestry Research and Development of Castilla-La Mancha (IRIAF) for providing financial support for this study.

References

Aavik, T., Reitalu, T., Kivastik, M., Reinula, I., Träger, S., Uuemaa, E., Barberis, M., Biere, A., Castro, S., Cousins, S.A.O., Csecserits, A., Dariotis, E., Fišer, Ž., Grzejszczak, G., Huu, C.N., Hool, K., Jacquemyn, H., Julien, M., Klisz, M., Kmoch, A., Krigas, N., Lengyel, A., Lenhard, M., Moges, D.M., Münzbergová, Z., Niinemets, Ü., Odé, B., Pánková, H., Pärtel, M., Pätsch, R., Petanidou, T., Plue, J., Puchałka, R., Rienks, F., Samartza, I., Sheard, J.K., Stojanova, B., Töpper, J.P., Tsoktouridis, G., Uzunov, S., Zobel, M., 2025. A pan-European citizen science study shows population size, climate and land use are related to biased morph ratios in the heterostylous plant primula veris (n/a). J. Ecol.. https://doi.org/10.1111/1365-2745.14477.

AEMET, 2012. Guía resumida del clima en España (1981-2010). Ministerio de Agricultura y Pesca, Alimentación y Medio Ambiente. https://doi.org/10.31978/281-12-011-4.

Ballero, M., Ariu, A., Falagiani Piu, P., G., 2003. Allergy to ailanthus altissima (tree of heaven) pollen. Allergy 58, 532–533. https://doi.org/10.1034/j.1398-9995.2003.00172.x.

Baptista, P., Costa, A.P., Simões, R., Amaral, M.E., 2014. Ailanthus altissima: an alternative fiber source for papermaking. Ind. Crops Prod. 52, 32–37. https://doi.org/10.1016/j.indcrop.2013.10.008.

Barrett, S.C.H., Hough, J., 2013. Sexual dimorphism in flowering plants. J. Exp. Bot. 64, 67–82. https://doi.org/10.1093/jxb/ers308.

Booth, T.H., 2016. Estimating potential range and hence climatic adaptability in selected tree species. For. Ecol. Manag. 366, 175–183. https://doi.org/10.1016/j.foreco.2016.02.009.

Cabra-Rivas, I., Saldaña, A., Castro-Díez, P., Gallien, L., 2016. A multi-scale approach to identify invasion drivers and invaders' future dynamics. Biol. Invasions 18, 411–426. https://doi.org/10.1007/s10530-015-1015-z.

Caramelo, D., Pedro, S.I., Marques, H., Simão, A.Y., Rosado, T., Barroca, C., Gominho, J., Anjos, O., Gallardo, E., 2021. Insights into the bioactivities and chemical analysis of ailanthus altissima (Mill.) swingle. Appl. Sci. 11, 11331. https://doi.org/10.3390/app112311331.

Castro-Diez, P., Valle, G., Gonzalez-Munoz, N., Alonso, A., 2014. Can the life-history strategy explain the success of the exotic trees ailanthus altissima and robinia pseudoacacia in iberian floodplain forests? PLoS One 9, e100254.

Clark, J., Wang, Y., August, P.V., 2014. Assessing current and projected suitable habitats for tree-of-heaven along the Appalachian trail. Philos. Trans. R. Soc. B Biol. Sci. 369, 20130192. https://doi.org/10.1098/rstb.2013.0192.

Constán-Nava, S., Bonet, A., Pastor, E., Lledó, M.J., 2010. Long-term control of the invasive tree ailanthus altissima: insights from Mediterranean protected forests. For. Ecol. Manag. 260, 1058–1064.

Cornelius, C., Petermeier, H., Estrella, N., Menzel, A., 2011. A comparison of methods to estimate seasonal phenological development from BBCH scale recording. Int. J. Biometeorol. 55, 867–877. https://doi.org/10.1007/s00484-011-0421-x.

de Groot, M., Kozamernik, E., Kermavnar, J., Kolšek, M., Marinšek, A., Nève Repe, A., Kutnar, L., 2024. Importance of habitat context in modelling risk maps for two established invasive alien plant species: the case of ailanthus altissima and phytolacca americana in Slovenia (Europe). Plants 13, 883. https://doi.org/10.3390/plants13060883.

De Martino, L., De Feo, V., 2008. Chemistry and biological activities of ailanthus altissima swingle: a review. Pharmacogn. Rev. 2, 339.
Delgado, P.M.H., Aranguren, M., Reig, C., Galvan, D.F., Mesejo, C., Fuentes, A.M., Sauco, V.G., Agustí, M., 2011. Phenological growth stages of mango (Mangifera indica L.) according to the BBCH scale. Sci. Hortic. 130, 536–540.
European Commission, 2020. List of invasive alien species of Union concern [WWW Document]. URL ⟨https://ec.europa.eu/environment/nature/invasivealien/list/index_en.htm⟩ (accessed 1.18.24).
Filippou, P., Bouchagier, P., Skotti, E., Fotopoulos, V., 2014. Proline and reactive oxygen/nitrogen species metabolism is involved in the tolerant response of the invasive plant species ailanthus altissima to drought and salinity. Environ. Exp. Bot. 97, 1–10.
Finn, G.A., Straszewski, A.E., Peterson, V., 2007. A general growth stage key for describing trees and woody plants. Ann. Appl. Biol. 151, 127–131.
Fournier, O., Alfredo, L., 1974. Un método cuantitativo para la medición de características fenológicas en árboles. Turrialba 24, 422–423.
Fridley, J.D., 2012. Extended leaf phenology and the autumn niche in deciduous forest invasions. Nature 485, 359–362.
Funk, J.L., Standish, R.J., Stock, W.D., Valladares, F., 2016. Plant functional traits of dominant native and invasive species in Mediterranean-climate ecosystems. Ecology 97, 75–83.
Gosper, C.R., 2004. Fruit characteristics of invasive bitou bush, chrysanthemoides monilifera (Asteraceae), and a comparison with co-occurring native plant species. Aust. J. Bot. 52, 223. https://doi.org/10.1071/BT03046.
Hu, S.Y., 1979. Ailanthus. Arnoldia 39, 29–50.
Hussen, A., 2021. Impact of temperature and relative humidity in quality and shelf life of mango fruit. Int. J. Hortic. Food Sci. 3, 46–50.
Jaryan, V., Uniyal, S.K., Gupta, R.C., Singh, R.D., 2014. Phenological documentation of an invasive species, sapium sebiferum (L.) roxb. Environ. Monit. Assess. 186, 4423–4429. https://doi.org/10.1007/s10661-014-3708-7.
Kaur, A., Batish, D.R., Kaur, S., Singh, H.P., Kohli, R.K., 2017. Phenological behaviour of parthenium hysterophorus in response to climatic variations according to the extended BBCH scale. Ann. Appl. Biol. 171, 316–326. https://doi.org/10.1111/aab.12374.
Ketsa, S., Pangkool, S., 1995. The effect of temperature and humidity on the ripening of durian fruits. J. Hortic. Sci. 70, 827–831.
Kheloufi, A., 2019. Inventory and distribution of Tree of Heaven (Ailanthus altissima) [WWW Document]. URL ⟨https://inaturalist.nz/projects/inventory-and-distribution-of-tree-of-heaven-ailanthus-altissima⟩.
Körner, C., 2021. The cold range limit of trees. Trends Ecol. Evol. 36, 979–989. https://doi.org/10.1016/j.tree.2021.06.011.
Kowarik, I., Säumel, I., 2007. Biological flora of central Europe: ailanthus altissima (Mill.) swingle. Perspect. Plant Ecol. Evol. Syst. 8, 207–237. https://doi.org/10.1016/j.ppees.2007.03.002.
Kuhn, R., 1957. Geholz-Winterschaden und ihre auswirkungen. Gartenamt 10, 201–202.
Kumar, A., Singh, S., Chand, H.B., Kumar, R., 2022. Phenological documentation of lantana camara L. Using modified BBCH scale in relation to climatic variables. Plant Sci. Today 9, 376–385. https://doi.org/10.14719/pst.1481.
Lediuk, K.D., Damascos, M.A., Puntieri, J.G., Svriz, M., 2014. Differences in phenology and fruit characteristic between invasive and native woody species favor exotic species invasiveness. Plant Ecol. 215, 1455–1467. https://doi.org/10.1007/s11258-014-0402-3.
Maan, I., Kaur, A., Singh, H.P., Batish, D.R., Kohli, R.K., 2020. Evaluating the role of phenology in managing urban invasions: a case study of broussonetia papyrifera. Urban For. Urban Green. 48, 126583. https://doi.org/10.1016/j.ufug.2020.126583.
Mabusela, M.M., Matsiliza-Mlathi, B., Kleynhans, R., 2024. Phenological growth stages of buddleja saligna willd. According to the BBCH scale. Plants 13, 3542. https://doi.org/10.3390/plants13243542.
Meier, U., 2001. Phenological growth stages. Mono dicotyledonous Plants Phenol. Integr. Environ. Sci. 39, 269–283.
Motti, R., Zotti, M., Bonanomi, G., Cozzolino, A., Stinca, A., Migliozzi, A., 2021. Climatic and anthropogenic factors affect ailanthus altissima invasion in a Mediterranean region. Plant Ecol. 222, 1347–1359. https://doi.org/10.1007/s11258-021-01183-9.
Nooteboom, H.P., 1962. Simaroubaceae Flora Males.
Paź-Dyderska, S., Ladach-Zajdler, A., Jagodziński, A.M., Dyderski, M.K., 2020. Landscape and parental tree availability drive spread of ailanthus altissima in the urban ecosystem of Poznań, Poland. Urban For. Urban Green. 56, 126868. https://doi.org/10.1016/j.ufug.2020.126868.
Puchałka, R., Klisz, M., Koniakin, S., Czortek, P., Dylewski, Ł., Paź-Dyderska, S., Vítková, M., Sádlo, J., Rašomavičius, V., Čarni, A., De Sanctis, M., Dyderski, M.K., 2022. Citizen science helps predictions of climate change impact on flowering phenology: a study on anemone nemorosa. Agric. For. Meteor. 325, 109133. https://doi.org/10.1016/j.agrformet.2022.109133.
Puchałka, R., Paź-Dyderska, S., Jagodziński, A.M., Sádlo, J., Vítková, M., Klisz, M., Koniakin, S., Prokopuk, Y., Netsvetov, M., Nicolescu, V.-N., Zlatanov, T., Mionskowski, M., Dyderski, M.K., 2023. Predicted range shifts of alien tree species in Europe. Agric. For. Meteor. 341, 109650. https://doi.org/10.1016/j.agrformet.2023.109650.
Pyšek, P., Hulme, P.E., Simberloff, D., Bacher, S., Blackburn, T.M., Carlton, J.T., Dawson, W., Essl, F., Foxcroft, L.C., Genovesi, P., Jeschke, J.M., Kühn, I., Liebhold, A.M., Mandrak, N.E., Meyerson, L.A., Pauchard, A., Pergl, J., Roy, H.E., Seebens, H., van Kleunen, M., Vilà, M., Wingfield, M.J., Richardson, D.M., 2020. Scientists' warning on invasive alien species. Biol. Rev. 95, 1511–1534. https://doi.org/10.1111/brv.12627.
R Core Team, 2025. A Language and Environment for Statistical Computing.
Ritonga, F.N., Zhou, D., Zhang, Y., Song, R., Li, C., Li, J., Gao, J., 2023. The roles of gibberellins in regulating leaf development. Plants 12, 1243. https://doi.org/10.3390/plants12061243.
Rivas-Martínez, S., Penas, Á., del Río, S., Díaz González, T.E., Rivas-Sáenz, S., 2017a. Bioclimatology of the iberian peninsula and the balearic islands. Veg. Iber. Penins. 29–80. https://doi.org/10.1007/978-3-319-54784-8_2.
Rivas-Martínez, S., Penas, Á., Díaz González, T.E., Cantó, P., del Río, S., Costa, J.C., Herrero, L., Molero, J., 2017b. Biogeographic units of the iberian peninsula and baelaric islands to district level. A concise synopsis. In: The Vegetation of the Iberian Peninsula, 1. Springer, pp. 131–188. https://doi.org/10.1007/978-3-319-54784-8_5.
Rojo, J., Pérez-Badia, R., 2014. Effects of topography and crown-exposure on olive tree phenology. Trees Struct. Funct. 28, 449–459. https://doi.org/10.1007/s00468-013-0962-1.
Sakar, E.H., El Yamani, M., Boussakouran, A., Rharrabti, Y., 2019. Codification and description of almond (Prunus dulcis) vegetative and reproductive phenology according to the extended BBCH scale. Sci. Hortic. 247, 224–234. https://doi.org/10.1016/J.SCIENTA.2018.12.024.
Sánchez-Salcedo, E.M., Martínez-Nicolás, J.J., Hernández, F., 2017. Phenological growth stages of mulberry tree (Morus sp.) codification and description according to the BBCH scale. Ann. Appl. Biol. 171, 441–450. https://doi.org/10.1111/aab.12386.
Scheerer, O., 1956. Winterschaden 1955/56. Gartenamt 9, 171–175.
Schwartz, M., 2013. Phenology: an integrative environmental science. Springer Netherlands, Dordrecht. https://doi.org/10.1007/978-94-007-6925-0.
Simberloff, D., Martin, J.-L., Genovesi, P., Maris, V., Wardle, D.A., Aronson, J., Courchamp, F., Galil, B., García-Berthou, E., Pascal, M., Pyšek, P., Sousa, R., Tabacchi, E., Vilà, M., 2013. Impacts of biological invasions: what's what and the way forward. Trends Ecol. Evol. 28, 58–66. https://doi.org/10.1016/j.tree.2012.07.013.
Sladonja, B., Sušek, M., Guillermic, J., 2015. Review on invasive tree of heaven (Ailanthus altissima (Mill.) Swingle) conflicting values: assessment of its ecosystem services and potential biological threat. Environ. Manag. 56, 1009–1034. https://doi.org/10.1007/S00267-015-0546-5/TABLES/3.
Soler, J., Izquierdo, J., 2024. The invasive ailanthus altissima: a biology, ecology, and control review. Plants 13, 931. https://doi.org/10.3390/plants13070931.
Thompson, E.J., 2021. A review of the classification and taxonomic and geographic distribution of cleistogamy in Australian grasses. Aust. J. Bot. 70, 63–101. https://doi.org/10.1071/BT20114.
Vilà, M., Trillo, A., Castro-Díez, P., Gallardo, B., Bacher, S., 2024. Field studies of the ecological impacts of invasive plants in Europe, 139-159 90, 139–159 NeoBiota 90. https://doi.org/10.3897/NEOBIOTA.90.112368.
Vitasse, Y., Lenz, A., Körnerr, C., 2014. The interaction between freezing tolerance and phenology in temperate deciduous trees. Front. Plant Sci. 5, 541. https://doi.org/10.3389/fpls.2014.00541.
Von der Lippe, M., Saumel, I., Kowarik, I., 2005. Cities as drivers for biological invasions-the role of urban climate and traffic. ERDEBerl. 136, 123.
Walker, G.A., Robertson, M.P., Gaertner, M., Gallien, L., Richardson, D.M., 2017. The potential range of ailanthus altissima (tree of heaven) in South Africa: the roles of climate, land use and disturbance. Biol. Invasions 19, 3675–3690. https://doi.org/10.1007/s10530-017-1597-8.
Werchan, M., Werchan, B., Bogawski, P., Mousavi, F., Metz, M., Bergmann, K.-C., 2024. An emerging aeroallergen in Europe: Tree-of-Heaven (Ailanthus altissima [Mill.] Swingle) inventory and pollen concentrations – taking a metropolitan region in Germany as an example. Sci. Total Environ. 930, 172519. https://doi.org/10.1016/j.scitotenv.2024.172519.
Yang, B., Cui, M., Du, Y., Ren, G., Li, J., Wang, C., Li, G., Dai, Z., Rutherford, S., Wan, J.S. H., Du, D., 2022. Influence of multiple global change drivers on plant invasion: additive effects are uncommon. Front. Plant Sci. 13, 1020621. https://doi.org/10.3389/fpls.2022.1020621.
Yang, Q., Gao, Y., Wu, X., Moriguchi, T., Bai, S., Teng, Y., 2021. Bud endodormancy in deciduous fruit trees: advances and prospects. Hortic. Res. 8, 139. https://doi.org/10.1038/s41438-021-00575-2.
Zadoks, J.C., Chang, T.T., Konzak, C.F., 1974. A decimal code for the growth stages of cereals. Weed Res 14, 415–421.
Zaraś-Januszkiewicz, E., Żarska, B., Fornal-Pieniak, B., Rosłon-Szeryńska, E., 2014. Phenological observations of ailanthus alitissima (Mill.) swingle at different urban areas. in: Plants in Urban Areas and Landscape. Slovak University of Agriculture in Nitra, pp. 35–39. https://doi.org/10.15414/2014.9788055212623.35-39.
Zaraś-Januszkiewicz, E.M., Rosłon-Szeryńska, E., Żarska, B., Fornal-Pieniak, B., 2020. The changes of phenological phases on the example of selected invasive species of trees. Plants Urban Areas Landsc. 86–92. https://doi.org/10.15414/PUAL/2020.86-92.